Development and Performance Evaluation of Impact and shock resistant wallpaper for Defense application

By

Dr. Kiran Shahapurkar

Dr. Venkatesh Chenrayan

Mr. Girmachew Ashegiri

A Final Research Report Submitted to Adama Science and Technology University

Adama, Ethiopia
March 2024

Table of content

Contents

List of Tables

List of Figures

Acknowledgement

First of all**,** we would like to thank the management of Adama Science and Technology University for their overviewed vision to elevate the university in to premier research center. We extend our thanks to the reviewers and research committee members for their valuable time devoted in the review process. We express our sincere thanks to the former Associate Dean for Technology Transfer Dr. Belay Birhane and present Associate Dean Dr. Shimles Lemma for their continuous and relentless encouragement and support to bring this project into a successful one. It is our responsibility to remind the efforts of technicians involved in the testing, evaluation, and assessment of experiments.

Abstract

The increasing demand for functionally graded material with minimum specific weight in every sector paves the way for novel materials development. The prime significance of this research is to develop the shock, impact-resistance and high strength lightweight material which can be recommended for construction and defense application. The performance evaluation of the developed composite against the impact and thermal loading is also an additional objective of the study. The woven Kevlar fabric was impregnated with varying weight percentages of Aluminium Oxynitride (ALON) particles infused epoxy matrix. Three different vol.% of ALON 5, 10, and 15 were used for the epoxy matrix preparation. The impact resistance of the material was examined through drop-weight impact testing along with necessary mechanical testing like tensile and flexural. The stiffness and damping capacity of the composite material were evaluated through Dynamic Mechanical Analysis (DMA). The scanning electron and optical microscope were employed to analyze the fracture mechanism and damage mechanism after the tensile, flexural and impact failures. The comprehensive study reveals an improvement in tensile yield strength of ALON 15 composites by 1.75 times as compared with ALON 0 whereas the ALON 15 specimen achieved a noticeable enhancement of 2.59 times in flexural strength than the flexural strength of the ALON-free specimen. The impact resistance, storage modulus, loss modulus, and damping characteristics of 15 vol.% ALON particles infused Kevlar epoxy composite also depict better response as compared with ALON-free Kevlar composite.

1. Introduction

1.1. Background of the study

Shock and impact resistance sheet materials have become increasingly important in a wide range of applications, including aerospace, automotive, construction, and consumer electronics. These materials are designed to protect against impact and shock, which can cause significant damage to equipment and structures, leading to costly repairs and downtime.

One of the earliest forms of shock-resistant sheet materials was laminated glass, which was first developed in the early 20th century. Laminated glass consists of two or more layers of glass with a layer of polyvinyl butyral (PVB) between them. When subjected to impact, the PVB layer holds the glass together, preventing it from shattering and reducing the risk of injury [1]. Today, laminated glass is used in a wide range of applications, from automotive windshields to hurricane-resistant windows [2]. In recent years, new types of shock and impact-resistant sheet materials have been developed using polymer composites. These materials consist of a matrix of polymer resin reinforced with fibers such as carbon or glass. The fibers help to distribute impact forces throughout the material, reducing the risk of damage. One popular type of shock and impact-resistant sheet material is polycarbonate [3]. Polycarbonate is a thermoplastic polymer that is highly impact-resistant and has excellent optical properties. It is commonly used in applications such as safety glasses, riot shields, and aircraft windows. Another type of shock-resistant sheet material is thermoplastic elastomer (TPE) [4]. TPE is a rubber-like material that can be molded into various shapes and has excellent impact resistance. It is commonly used in applications such as cell phone cases, power tool grips, and automotive bumpers.

In addition to polycarbonate and TPE, there are a variety of other shock and impact-resistant sheet materials available, including acrylic, polyurethane, and silicone. These materials have different properties and are used in a range of applications, from bulletproof vests to protective cases for electronic devices. Overall, the development of shock and impact-resistant sheet materials has been driven by the need to protect against

impact and shock in a wide range of applications. Advances in materials science and manufacturing processes have led to the development of new and improved materials that offer better performance and durability, helping to keep equipment and structures safe and protected.

1.2. Problem statement

In the war field, it is necessary to create a temporary shelter either by digging a foxhole or building a temporary wall by stacking sandbags to a certain height. In some cases, abandoned buildings are also used as temporary combat shelters to safeguard the soldiers. However, a natural constraint with the usage of buildings for this purpose is the incapability of withstanding shockwaves during ballistic attacks like Fullmetal jacket (FMJ) resulting in the imploding of walls and sending pieces of rocks and mortar that cause severe injuries to the soldiers. The crater developed due to implode causes the wall to fail further. Therefore, it is the fundamental technique necessary to fortify the building with advanced shock and impact-resistant materials. Moreover, in the war field, it is of utmost importance to protect the defense equipment, including electronic systems, communication devices, sensitive instruments, and military vehicles carrying weapons from damage caused by impact, vibration, or shock. The present research aims to develop Aluminium Oxynitride (ALON) filled epoxy composite sheet reinforced with Kevlar fabric, flexible to fasten over the inside of any enclosure.

1.3. Objectives

The general objective of this project is to fabricate, mechanical characterization and performance evaluation of shock and impact-resistant polymer composite sheets for defense applications.

The specific objectives derived as follows,

- Preparation of Aluminum Oxy Nitride reinforced epoxy resin slurry.
- Development of composite wall paper reinforced with Kevlar fabric using hand layup technique
- Morphological characterization for homogeneity and elemental composition.

- Evaluation of mechanical properties like tensile strength, hardness and flexural rigidity
- Experimental evaluation of impact resistance through drop weight impact test.
- Thermo-gravimetric and Differential Calorimetric analysis to study the thermal behavior of composite sheet.
- Development of sticking agent and application on one side of the ballistic sheet.

1.4. Significance of the study

The impact, shock wave, and vibrations are the predominant external catalysts that disturb the structure's integrity and transform into failure. These impacts, shock waves, and vibrations are uncertain to predict and their effect is linearly related to their frequency. The structural materials used whether for domestic or defense applications are expected to perform well despite these difficulties. The present work targets to develop the ALON-filled epoxy-based composite sheet reinforced with Kevlar fabric to fortify the structures from unpredicted impacts and shock waves. To uphold the assured performance of developed shock-resistant epoxy composite sheets against uncertain impacts and shocks, the epoxy composite sheets are experimentally evaluated for their flexural rigidity, impact rigidity, and damping ability at elevated temperatures followed by necessary micrographic observation to validate the deformation physics.

2. Literature review

P.N.B. Reis et.al [5] conducted an experiment with two different Kevlar mat-impregnated epoxy resin reinforced with cork powder and nano clay. The authors executed a drop weight impact test with varying energy 6, 12 and 21 J. The report concluded the finding that the nano clay-infused Kevlar epoxy composite possesses greater impact resistance than the cork powder-infused Kevlar composite, subsequently, it experienced lesser damage. Sushant Sharma et.al [6] carried out the study to develop the Kevlar mat epoxy composite reinforced with three different proportions of CNT (0.1, 0.2, and 0.3%). The various mechanical assessments like tensile strength, flexural strength and storage modulus were done experimentally. The authors concluded that the multi-fold increment is achieved with the inclusion of 0.3 % CNT in tensile modulus,

flexural modulus and storage modulus. The greater improvement was attained by improving interfacial interaction between epoxy and kevlar through CNT.

Youjiang Wang et.al. [7] developed the novel Kevlar 49 and glass fibre woven epoxy composite laminate. Apart from the usual tensile, flexural, compressive and shear mode investigation, the authors attempted to evaluate the interlaminar fracture behaviour with the help of a Double Cantilever Beam (DCB) loading. Clement Audibert et.al. [8] performed the comprehensive tensile and flexural examination on flex fiber–kevlar fiber woven epoxy composite. The three-point bending test was also simulated through a numerical package to validate the experimental results. The authors reported an intermediate mechanical property for a hybrid composite between flax and Kevlar epoxy composite. Zuo Tai Zhang et.al. [9] have conducted an investigation study on ALON-TiN composite by infusing 3 -15 % of TiN and they reported a significant improvement in oxidation and wear resistance with a noticeable tensile strength of 487 MPa. The E-glass reinforced vinyl ester and urethane panels were fabricated by Michael Hebert et.al to evaluate their performance against shock and impact loading. The authors concluded the improvement in the performance of vinyl easter against both shock and impact loading. Post-mortem damage assessment through visual image processing confirms the minimum damage with sustained loading.

Ariff Farhan Mohd Nor et .al [10] executed drop weight impact assessment on CNT-reinforced bamboo-glass fiber hybrid polymer composite. They conducted Low velocity Impact (LVI) and Compression After Impact (CAI) tests to evaluate the performance of the composite. The report explored the 25.67% improvement achieved for 0.5% CNT reinforcement towards the CAI strength. Avila et.al. [11] fabricated the nano clay-filled epoxy composite impregnated by glass fiber. The inclusion of nano clay varied like 1, 2, 5 and 10 % and three levels of impact energy 20, 60, and 80J were followed to conduct the drop weight impact examination. The authors declared that the stiffness and impact resistance of 5% nano clay composite is improved in a significant way.

Pragati Priyanka et.al [12] carried out the dynamic mechanical analysis on Kevlar and carbon-kevlar hybrid epoxy composite. The two different kevlar composites were

pressed into dynamic mechanical analysis under three different tensile, compression and flexural loadings. The report manifested a greater improvement in storage modulus, loss modulus, and damping characteristics of the twill-weaved carbon-Kevlar epoxy composite than the plain-weaved carbon-Kevlar epoxy composite and monolithic Kevlar composite.

The investigation of the influence of graphene and hexagonal-boron carbide (h-BN) on carbon, Kevlar composite and hybrid composite was executed by Srivatsava Madarvoni et.al.[13]. The research conclusion stated that 0.5% graphene and h-BN reinforced glass fiber composite register a 49% increase in storage modulus and a 38% improvement in loss modulus. The authors recommend the hybrid composite for compression and damping application. Sarasini et.al [14] experimented basalt-carbon fibre hybrid laminate against low velocity impact, the authors followed two different stackings: alternate sequence of caron and basalt fibre and carbon-carbon sequence. The damage assessment and flexural test results after the impact reveals that the basalt – carbon hybrid laminates possess the higher capacity of absorbing impact energy than carbon-carbon stackings. Based on the literature it was inferred that the ALON particles are very much suitable for high strength applications. However, as far as the authors knowledge there are no studies reported on the use of ALON particles with Kevlar-epoxy composites. Additionally, Kevlar-epoxy sheet for ballistic impacts are not explored and thereby the present work focussed on the use of ALON particles in Kevlar-epoxy composites.

3. **Methodology**

3.1. Materials

LY-556 epoxy with HY-951 hardener was procured from Metal Mart, Coimbatore. A Kevlar fabric of 1x1m dimensions with a specification PT 003 was procured from Scientific suppliers, Chennai, India. The specification of the Kevlar fabric is shown **Table 1.** It is woven fabric using warp and weft yarns made up of Kevlar from the DuPont trademark.

Table 1. Specification of Kevlar fabric

Class	Weight (gm/m^2)	Width (cm)	Weave style	Thickness (mm)
PTOO3	200	30	Twill	0.26

The Aluminium oxynitride (ALON) particles were purchased from Metal Mart, Coimbatore, India. The supplier document confirms the particle size to the range of 50 to 60 μm. The mechanical properties of ALON are furnished in **Table 2**

Table 2. Mechanical properties of ALON

Compressive strength	2.58 GPa
Shear modulus	134 GPa
Young's modulus	333 GPa
Flexural strength	0.35-0.75 GPa
Knop hardness	1750 kg/mm^2
Poisson's ratio	0.24

3.2. Fabrication of Kevlar-ALON reinforced epoxy sheets

The Kevlar fabric was cleaned with a soft brush and completely washed in acetone to remove embedded impurities and the ALON was also rinsed with acetone. Then the Kevlar fabric was cut into 300×300 mm to suit the mold. The bottom surface of the mold was applied with wax for easy removal of the specimen. The three different volume percentages of 5, 10 and 15 of ALON were followed to fabricate the specimen [15]. Initially, the premeasured quantity of ALON particles was added with the measured

volume of epoxy and the solution was fed into magnetic sonication for 45 minutes at 200 rpm. Then, 10 % wt. of hardener was also added to the mixture. Part of the solution was poured on the mold followed by a laying of pre-truncated Kevlar fabric. The rest of the solution was also poured over the Kevlar mat. Then, the roller brush was used to roll and squeeze out the surplus epoxy mixture. The small size roller was employed to roll on the corners of the mold. The entire mold set-up was allowed to cure for 24 hrs. Finally, specimens were withdrawn from the mold by dismantling the bolts available on the boundary bars. The different sizes of the specimens required for tensile, flexural, drop weight impact, and Dynamic Mechanical Analysis (DMA) tests as per ASTM standards were machined using abrasive water jet machining.

3.3. Tensile testing

ASTM 638-14 standard was followed to conduct the tensile test. A universal testing machine (ZO20 Zwick Roell, United States) was employed to carry out the testing of samples. A 165mm length and 19 mm width dimensioned tensile test coupon with a dog bone structure are as shown in **Figure 1 (a)**. Out of 165 mm, 115 mm was utilized for examination length and the rest of the 50 mm was used as gauge length. The steady and slow speed at the rate of 5 mm/min was maintained until the coupon becomes failed. The details of the load and its corresponding displacement were recorded from the output window and were utilized to construct the stress-strain curve.

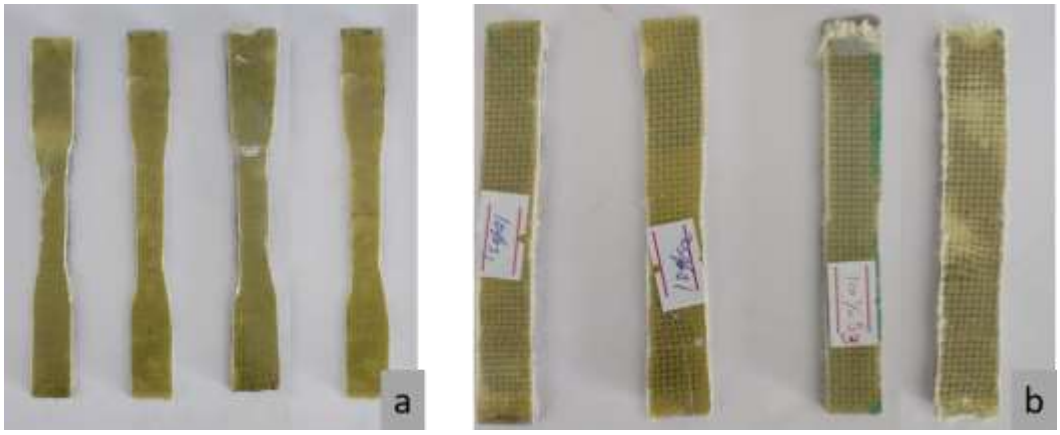

Figure 1 Test specimens image (a) Tensile test (b) Flexural test

3.4. Flexural testing

ASTM790-10 [15] standard was followed to conduct the flexural test. The same universal testing machine set-up was employed to execute the necessary flexural testing. A 127 mm length and 12.7 mm width dimension as shown in **Figure 1 (b)** were followed to align with the standard. The steady movement of the crosshead was maintained at 1.8 mm/min until the specimen fractured. The load and displacement data obtained from the flexural testing were utilized to calculate the flexural strength and modulus with the help of the following equation [15]

Flexural strength (= —— (1)

Flexural Modulus (—— (2)

Where the notations are briefed as given in Table 3.

Table 3. Notations in flexural equations

W	Maximum load
m	Slope of the stress–strain curve
L	Length of the coupon
b	Width of the coupon
t	Thickness of the coupon

3.5. Drop weight impact testing

ASTM-D7136 [11] standard was followed to conduct the drop weight impact test. A drop weight impact testing set-up (Imatek 1M10) was employed to execute the testing. A specimen size of 150 mm in length and 100 mm in width was maintained to cope with ASTM standards. A 25 mm of support length was secured by a toggle clamp with rubber edges to avoid the rebound. An impact ball of 2 kg mass was allowed to fall from a height of 2 m on the positioned specimen. The final velocity with which it contacts the first layer was known as 6.21 m/s. The data acquired from the load cell fixed on the crosshead during impact was utilized for insight into the damage mechanism.

Furthermore, the data were used to plot the load, displacement and energy versus time graph with the help of the equation follows [16].

Velocity distribution with respect to time, (∫ ((3)

Displacement propagation with respect to time (∫ ((4)

Energy absorption with respect to time (∫ (—(((5)

Results and discussion

4.1. Characterization

Figure 2 depicts the micrograph of a polymer composite composed of Kevlar fabric and ALON particles. The SEM micrograph assures the uniform dispersion of the ALON particles over the Kevlar fabric and matrix.

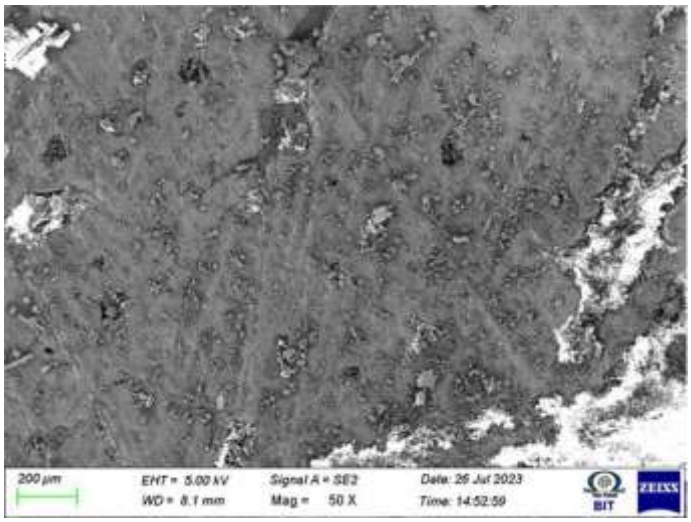

Figure 2. SEM micrograph of Kevlar-ALON composite sheet

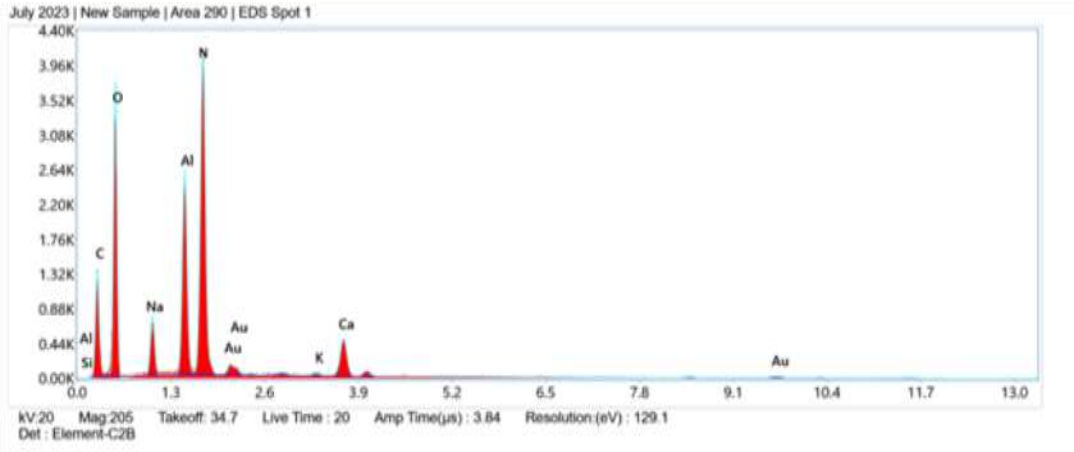

Figure 3. Elemental analysis of composite through EDAX.

Table 4. Elemental composition of composites

Element	Weight %	Atomic %
C K	20.59	30.84
O K	41.89	47.11
Na K	4.99	3.91
Al K	9.35	6.24
N K	15.25	9.77
K K	0.28	0.13
Ca K	3.67	1.65
Au L	3.99	0.36

Figure 3 shows the elemental analysis of the Kevlar-ALON polymer composite. The results endorse the existence of important elements having main peaks of aluminum, nitrogen and oxygen. Table 4 depicts the elemental composition of all the elements present in the composites.

4.2. Tensile behavior

The stress-strain curve plotted from the data acquired from the tensile testing of four different proportions of ALON is shown in **Figure 4.**

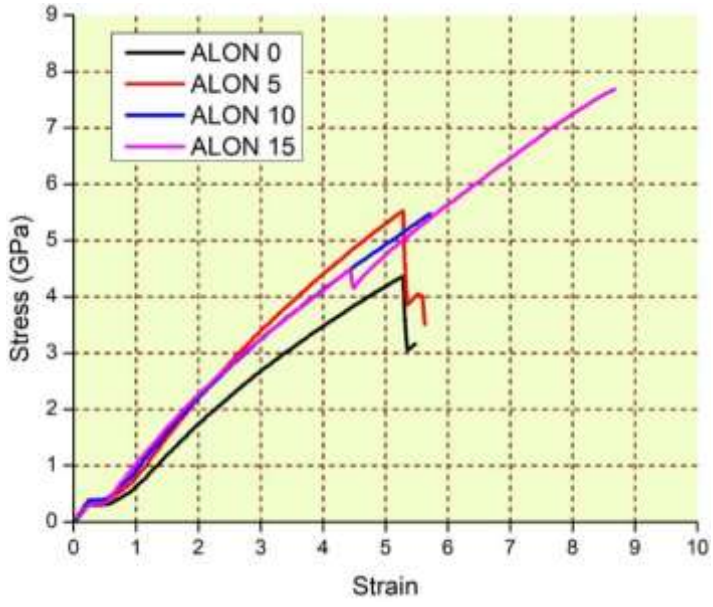

Figure 4. Stress-strain plot from tensile test

It is vivid from the results that the Kevlar epoxy sheet with 15 vol.% of ALON particles experiences the extreme flexibility against the tensile loading. The ALON free Kevlar epoxy specimen achieved the earliest failure by attaining a maximum stress of 4.37 GPa, whereas 15 vol.% inclusion of ALON particles enhance the resistance against the loading to the tune of 7.68 GPa. ALON 15 specimen postpones its failure with significant elastic straining. It is observed from the results that both ALON 5 and ALON 10 also recorded a premature failure than ALON 15. The failure mechanism manifests the importance of the inclusion of ALON. With the increased tensile load, the delamination of epoxy from the Kevlar fabric is observed, and the loading continues, the brittle failure is succumbed by epoxy and the plastic failure is succumbed by Kevlar fabric. The higher inclusion of ALON particles makes a bridge between the matrix material and Kevlar particles to retard the delamination effect, thereby improving load bearing capacity with considerable elastic strain. The tensile study reveals a 1.75 times improvement in yield tensile stress and strain for the ALON-rich epoxy Kevlar specimen in comparison with the ALON-free epoxy Kevlar composite specimen.

4.2.1. Tensile Modulus and Strength

The tensile modulus and strength is the key indicator for the mechanical behaviour of the hybrid composite sheet against the functional loading. The tensile modulus obtained from the experimental results has been presented in **Figure 5.** The bar chart annunciates the increasing trend of tensile modulus for every incremental vol.% of ALON. The comparison confirms the substantial increment of tensile modulus for the ALON 15 specimen to the tune of 1.57 times than the ALON 0. This significant improvement is attributed to the excellent load-transferring capacity of hard particles ALON [17]. The strengthened Kevlar fabric contributes to the noticeable jump in tensile modulus for Kevlar fabric-impregnated epoxy specimens irrespective of the inclusion of external particles. But the variation in tensile modulus among the specimens is primarily due to the variation in the inclusion of ALON particles. Similar results of increasing reinforcing agent improve the property [18] was reported. From the stress-strain plot, the sustained elastic deformation is observed for a higher level of the inclusion of ALON particles due to the load bearing capacity of ALON particles. The good bonding of

ALON particles between the epoxy matrix and Kevlar fabric plays an instrumental role to decelerate the elastic strain by sustaining more load.

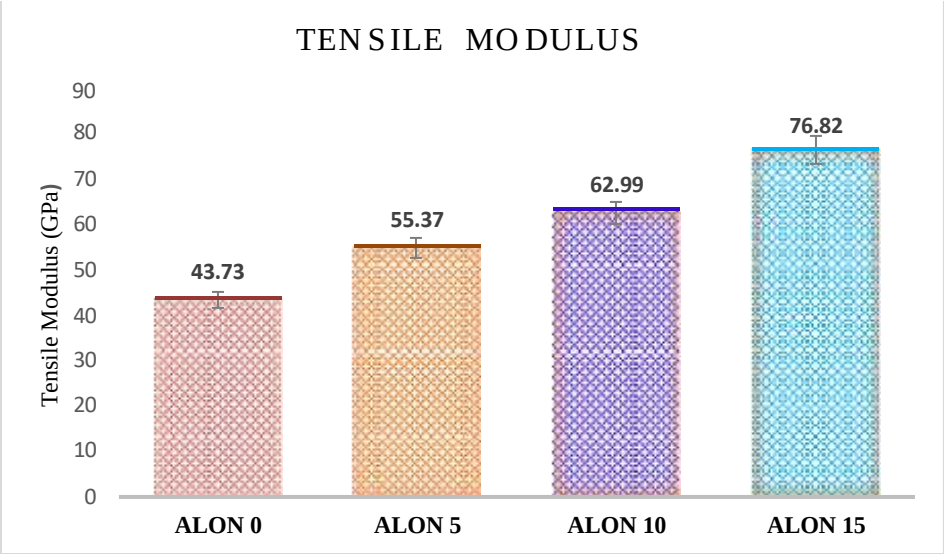

Figure 5. Comparison bar chart of tensile modulus of Kevlar-ALON composite

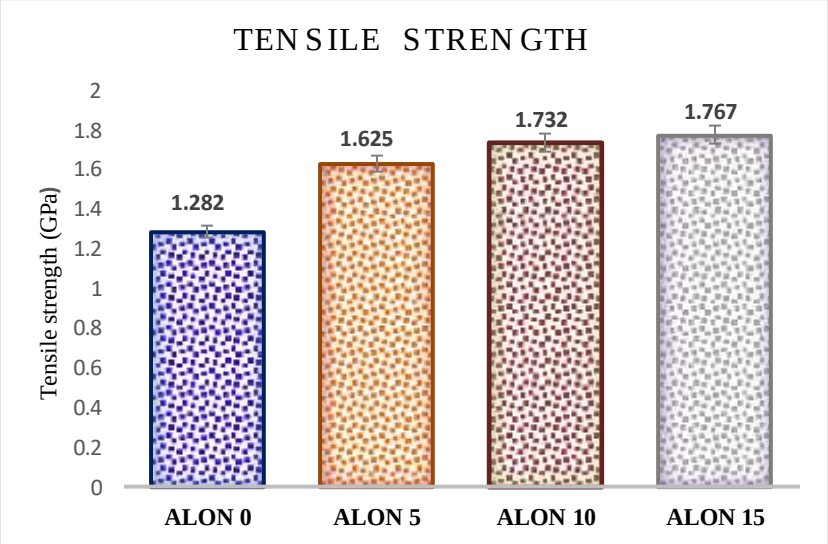

Figure 6. Comparison bar chart of tensile strength of Kevlar-ALON composite

Figure 6 depicts the tensile strength observed during the tensile loading experiment. The tensile strength is the dependent property index of the stress developed. Therefore, a similar trend in the stress-strain plot is mimicked in the tensile strength chart. Nearly 37 % of improvement is recorded for the specimen with 15 vol.% inclusion of ALON in comparison with ALON-free specimen. Completely dispersed ALON

particles within the epoxy and Kevlar fabric pose an obstacle to the movement of polymer molecules, thereby exhibiting more stiffness against load. The delayed response of polymer molecules against the load increases the maximum stress which in turn reflects in the improvement of tensile strength.

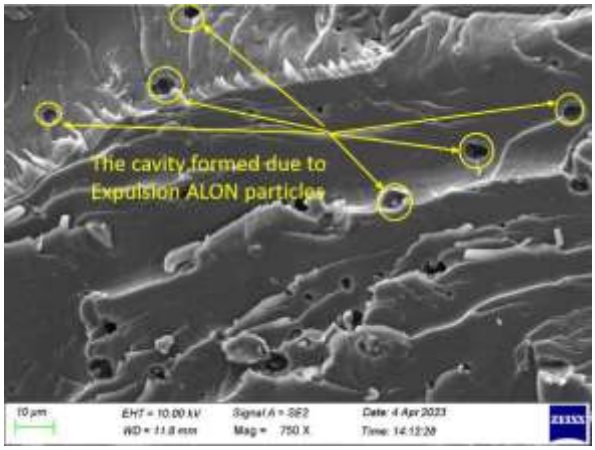

Figure 7. Fractured micro graph at delaminated region

Figure 7 shows the fractured micrograph observed at delaminated region during tensile fracture. Both the tensile modulus and tensile strength results affirm the similar behavior of increased resistance against loading for the increased level of ALON particles. The failure is recorded for all the specimens followed by the delamination of matrix material from the Kevlar fabric. It is comprehended from the results that the delayed delamination postpones the failure, and hence the improvement in both the property indices. The delayed delamination is promoted by the good bonding of ALON particles with the Kevlar fabric and epoxy matrix. The cavity formed as shown in **Figure 7** due to the expulsion of ALON particles explores the delamination-driven fracture mechanism.

4.3. Flexural behavior

4.3.1. Stress-strain Phenomenon

The flexural stress-strain plot shown in **Figure 8** is found to be more useful to comprehend the flexural characteristic of the Kevlar-ALON composite specimen. It is we**l** understood from the plot's trend that the linear relationship between stress and strain exhibits elastic bending. However, the three-point bending causes different stresses in

nature: the upper layer contact with the loading bar is subject to compressive stress and the bottom layer is subject to tensile stress [19]. Since all the specimens are reinforced with Kevlar fabric, the variation in flexural stress recorded is attributed to the inclusion of the ALON particles in varying vol.%. The specimen with minimum and nil vol.% of ALON particles experienced catastrophic failure with lesser stress development and displacement. But, the higher vol.% of ALON particles pose significant resistance against bending by deforming in a plastic manner. The flexural results reveal that the ALON 10 specimen withstands a bending load 2.84 times more than that of the ALON 0 specimen succumbs. The ALON 15 specimen manifests its superior stiffness by experiencing the highest deformation of 27 mm before failure against the peak load of 118 kN. The ALON 15 specimen records 80% more displacement at 162 % excess load than that of the ALON 0 experienced. The sustaining ability of the ALON 15 specimen against bending failure explores the influence of sophisticate (high impact resistance and ballistic) ALON particles. The fractured specimens confirm the failure prompted by delamination. Initial delamination and brittle failure occurred to the ALON 0 specimen owing to faster dislocation of polymer molecules under both tensile and compressive stresses [20] . This immediate response of the polymer molecules hinders the plastic deformation thereby inducing earlier failure. The higher dispersion of ALON particles in ALON 10 and 15 specimens impede the movement of the polymer chain, and in turn, the induced resistance reinforces the specimen to sustain more flexural stress.

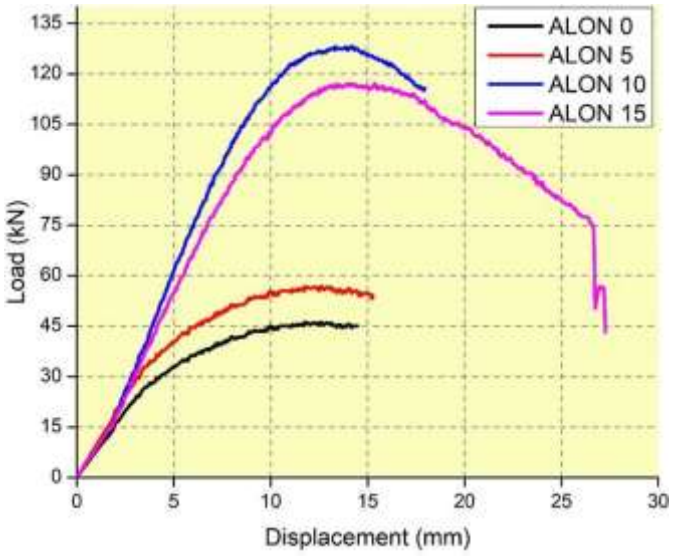

Figure 8. Flexural stress -strain plot for Kevlar-ALON composite

4.3.2. Flexural strength

Flexural strength is an indicator of maximum stress with which the material can sustain the transverse load before being failure. The transverse load with simply supported beam system causes a combined stress of tension and compression. Usually, these combined stresses cause a delamination effect for continuous fiber reinforced polymer composite.

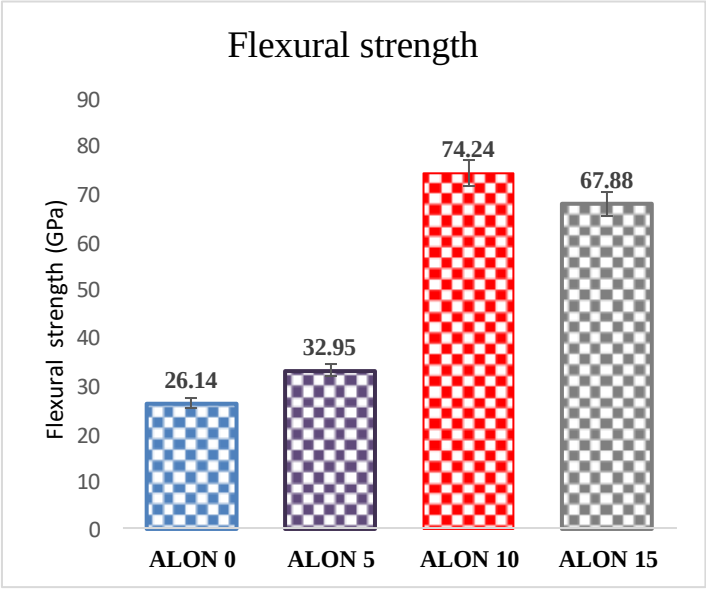

Figure 9. Comparison bar chart of flexural strength of Kevlar-ALON composite

Figure 9 depicts the flexural strength recorded at three point bending for the four different Kevlar-ALON polymer composite. The similar increasing trend with the increasing in ALON particles is reflected despite the ALON 10 specimen records the maximum stress than the ALON 15. The higher quantity of ALON (15 vol.%) dispersed homogeneously and bonded in fair manner resists the delamination and postpones the failure. Though the ALON 10 records the maximum stress, its failure is very earlier than the ALON 15 owing to its insufficiency in load bearing. The comparison clearly comprehends that the ALON 15 specimen achieved a noticeable enhancement of 2.59 times in flexural strength than the flexural strength of the ALON-free specimen. The strength of ALON particles and their tendency to arrest the movement of the polymer chain is the predominant reason for the increment in flexural strength.

4.3.3. Flexural Modulus

The flexural modulus is a simple representation of stiffness and is an outcome of the slope of the bending stress–strain curve. Usually, the materials possessing poorer response in deformation hold the higher value of flexural modulus.

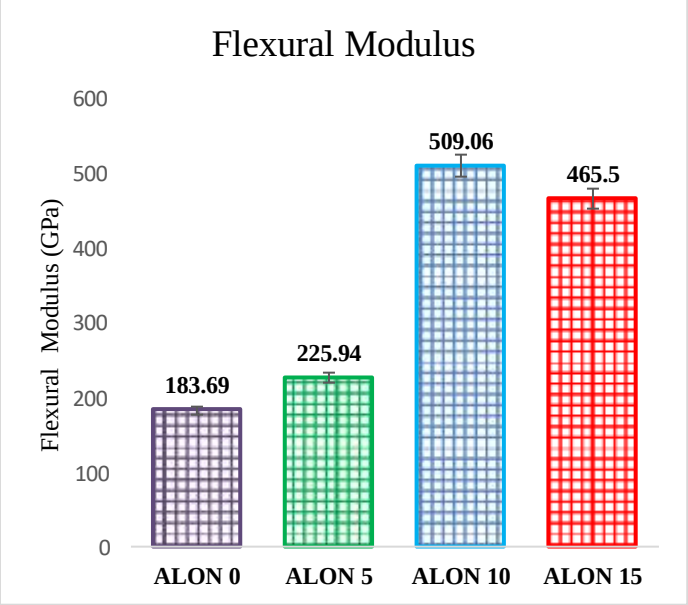

Figure 10. Comparison bar chart of tensile modulus of Kevlar-ALON composite

The flexural modulus is a relative property of flexural strength; hence the trends are in similar with the flexural strength. The increment in modulus for the increased

inclusion of the ALON particles is attributed to higher young's modulus value of the ALON particles. Moreover deformation retention by withstanding the transverse load is attained due to the load transfer ability of the ALON particles between matrix material and Kevlar fabric[21]. ALON particles are responsible to enhance the stiffness by decelerating the elastic strain. This excellent strength and homogeneous dispersion of ALON particles escalate the tensile modulus of ALON 15 to 1.53 times higher than ALON-free specimen as seen in **Figure 10.**

4.3.4. Fracture analysis

The additional strength imparted by the inclusion of ALON particles can be well understood by the fracture mechanism captured through SEM micrographs as shown in **Figure 11.** The significant improvement in both tensile and flexural strength by the higher level of ALON particle inclusion is clearly demonstrated in **Figure 11 (a).** It is clearly visible that the part of the fabric fiber are firmly bonded with the matrix because of more quantity of ALON particle in the ALON 15 specimen, despite its failure with noticeable delamination. The premature failure of the ALON-free specimen can be comprehended with the different stages of failure: fiber pull-out, delamination and fracture. It is realized from the experimental results that the failure is prompted by the delamination effect as shown in **Figure 11 (b).**

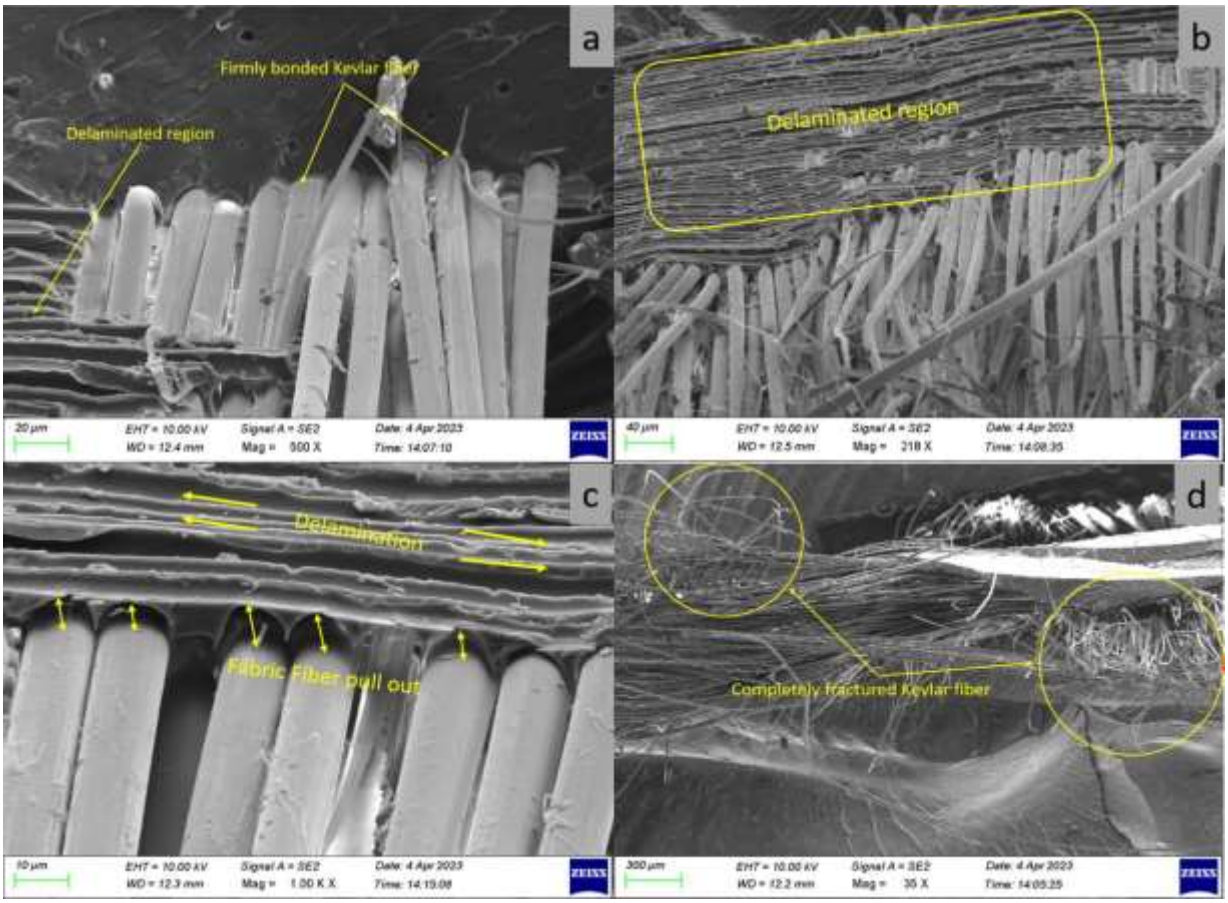

Figure 11. Fractured micrograph post flexural test (a) Fractured surface of ALON 15 (b) Fractured surface of ALON 5 (c) fractured surface of ALON 0 (D) Fabric failure of ALON 0

However, the delamination is prompted by the individual fabric fiber pull out from the matrix as shown in **Figure 11 (c).** The collective pullout of many fibers from the matrix is considered to be a delamination [22]. Therefore, the retention of fabric fiber within the matrix is a scientific way to retard the fiber pullout, thereby minimizing the delamination effect. The importance of the inclusion of ALON particles is realized through their bonding and load-sharing capacity to retain the fabric fiber within the matrix thereby postponing the failure. This phenomenon manifests the stiffness of the composite specimen and the reason behind the increment of both tensile and flexural modulus. The extended load after the delamination of ALON- free specimen is subject to the complete failure of Kevlar fabric as shown in **Figure 11 (d).**

4.5. Impact analysis and damage assessment

A deep insight into the impact behavior, resistance nature and the damage assessment are being discussed with the drop weight impact results. The phenomenon of impact resistance and damage mechanism is explored through load vs time, displacement vs time, velocity vs time and energy vs time plotting.

4.5.1. Force vs time

Figure 12 shows the recorded the resistance force for the applied impact with respect to time. The trend of the graph from the data obtained for the four different variant of ALON specimens implies that the peak force reached at the point of impact (damage) and starts to diminish to zero.

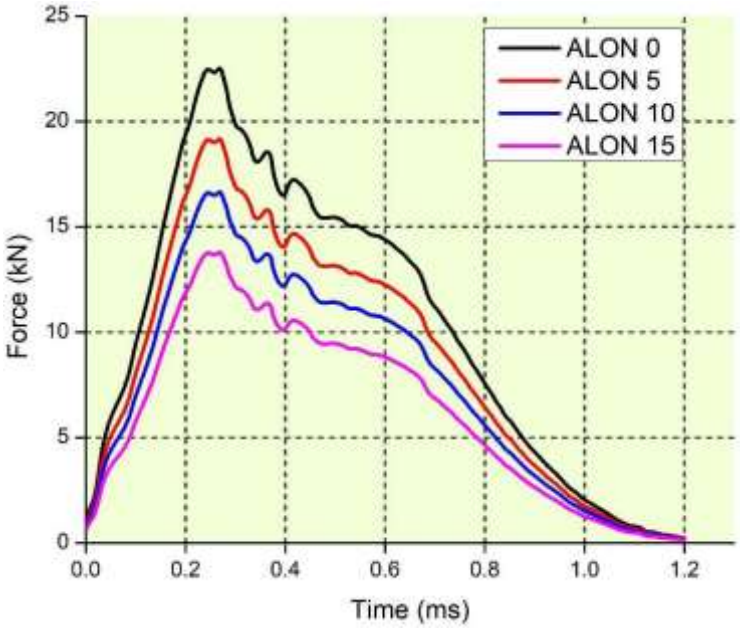

Figure 12. Force vs Time plot

The behavior of all the specimen seems to be uniform except their individual peak force. Since it is well understood from the tensile testing that the increase in ALON content increases the stiffness of the material. The higher stiffness material experiences the lower in fracture toughness and damping [5]. It is evident from the results that the ALON 15 records the lesser impact force 13.831 kN, whereas the ALON 0 records a higher impact force of 22.587 kN. The declining trend of force is recognized due to the

resulting strain rate effect and frictional effect between the ball and specimen surfaces. The notable improvement in impact force for ALON 15 specimen is attributed to the higher stiffness caused by the inclusion of more ALON particles.

4.5.2. Velocity vs time

As per the drop weight testing parameters, the initial velocity with which the ball hits on the surface of the specimen was kept constant (6.28 m/s) for all the specimens. However, the response of each specimen with the impinging velocity differs according to variation in ALON quantity.

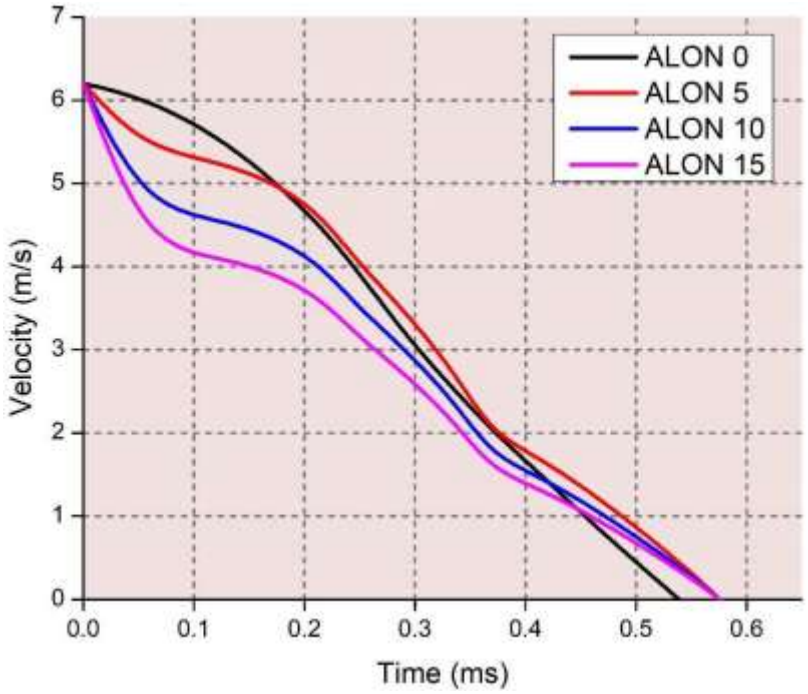

Figure 13. Velocity vs Time plot

Figure 13 depicts the velocity response of the specimens. The velocity becomes zero after impacting and causing damage to the specimen. The effect of damage is more for the ALON 0 specimen than the ALON 15, because the damage effect is augmented due to the sustained velocity phenomenon. However, the ALON filled specimen experiences the sharp fall in velocity at 0.1 ms itself. The damage effect seems to be lesser for the ALON rich specimen owing to the velocity collapse instigated by the elastic energy obtained from the impact strength of the ALON.

4.5.3. Displacement vs Time

The response of the composite specimen against the impact is considered to be a failure like deformation, displacement, and penetration. **Figure 14** depicts the displacement or damage of the specimen as a function of ALON inclusion.

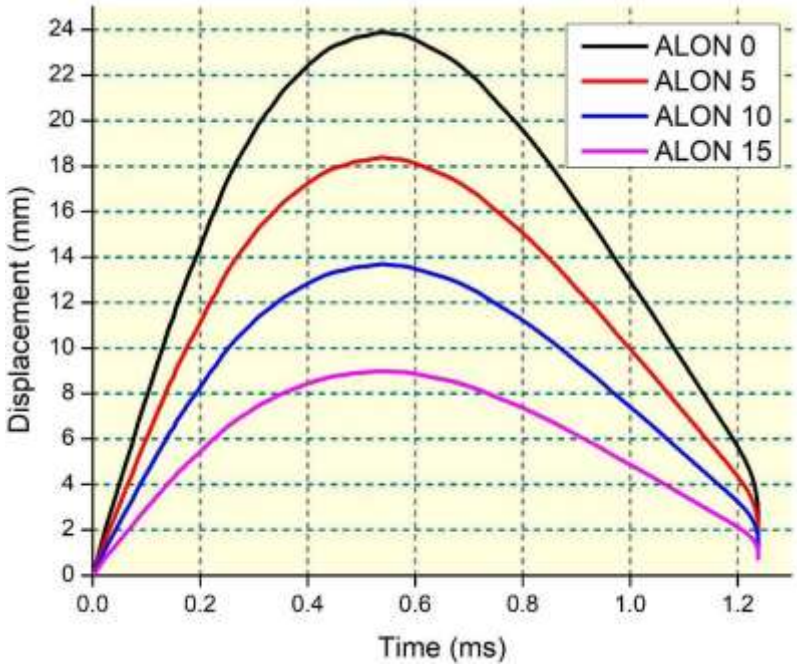

Figure 14. Displacement vs time plot

From the graph, it can be visible that the velocity is steadily increasing until the maximum damage and declining to zero. The maximum damage is observed for ALON – free specimen as 16 mm. The improved stiffness offered by the ALON particles, and their impact resistance property safeguards the ALON 15 specimen with lesser damage 56.25 % than that of ALON 0.

4.5.4. Energy vs Time

The kinetic energy developed during the impact is the prime catalyst to induce the damage. The energy impacted on the surface of the specimen is learnt to be disbursed in to two category: Part of the energy is spent for rebounding the ball and rest of the energy is absorbed by the specimen [23]. **Figure 15** manifests the decomposition of impacted energy as the function of ALON inclusion. The non-noticeable rebounding is recorded by consuming elastic energy, which has decomposed from the incident energy due to the

stiffness of the material. The energy absorbed by the specimen is responsible for the damage mechanism. The impact-resistant material is capable to decompose the incident energy to more elastic nature than its capacity to absorb. The energy-time plot reveals the ALON 15 specimen succumbs to minimum damage than any other variant of the Kevlar composite. The higher stiffness induced by the ALON-rich fillers diverts the incident energy to elastic energy thereby rebounding the ball. The energy absorbed by the specimen is comparatively lesser than all other specimens, resulting in minimum damage.

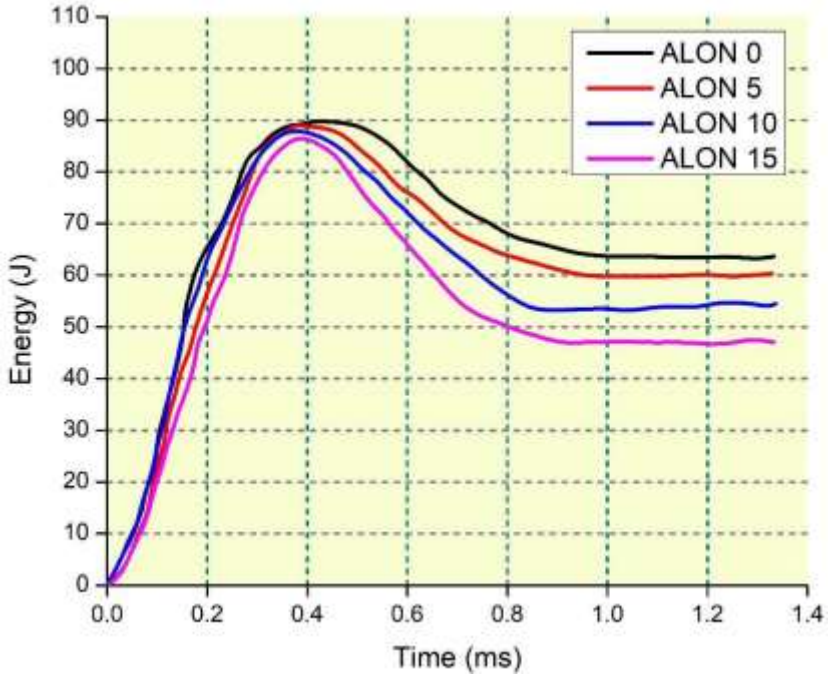

Figure 15. Energy-time plot

4.5.5. Damage assessment

The damage is a catastrophic outcome of impact energy, the damage study reveals the behavior and mechanism which initiate the failure. From the earlier discussion, it is quite obvious that the quantity of ALON inclusion dictates the impact force, velocity response, and energy decomposition. The failure of specimen is also a collective outcome of these impact parameters. The primary mechanism which initiate the damage is a delamination. The macro images of fractured specimen affirms that the delamination is an outcome of brittle failure of the matrix material, when it is subjected to impact loading. For the initial moment, the surface of the specimen experiences the brittle

failure, followed by a delamination. Further impact energy absorbed by the specimen initiate a crack in the Kevlar fabric fiber. Since it is non-perforating testing, the area of indentation of individual specimen varies according to their ALON inclusion. The marked and highlighted area in **Figure 16 (a) – (d)** reveals the brittle failure of the epoxy matrix and the measurement of indentation.

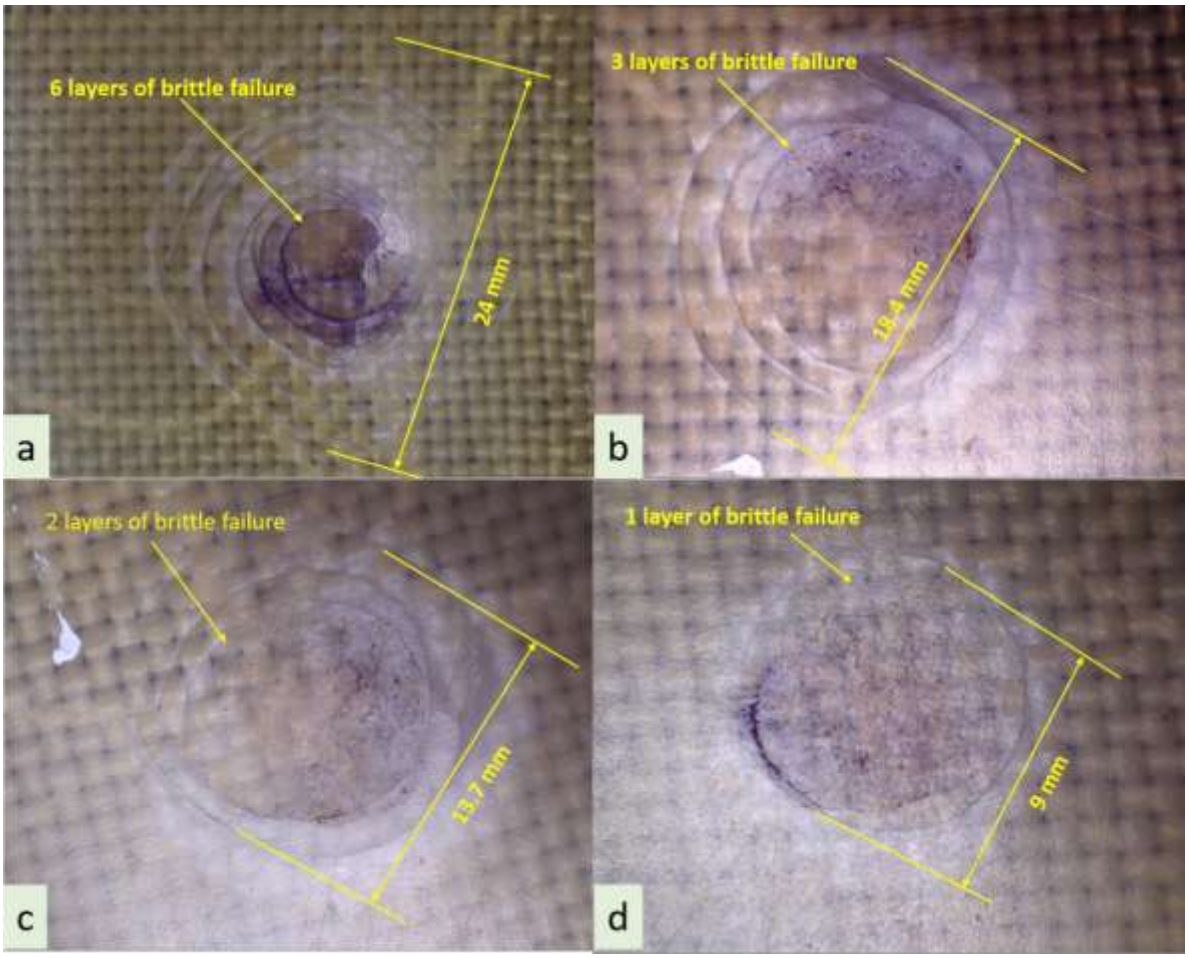

Figure 16. Damage assessment (a) ALON 0-Kevlar (b) ALON 5-Kevlar (c) ALON 10-Kevlar (d) ALON 15-Kevlar

In comparison with **Figure 16 (a) and Figure 16 (d),** the ALON 0 specimen shown in **Figure 16 (a)** succumbs to higher percentage failure by absorbing most of the impacted energy because of its lack of stiffness. The surface of the epoxy material suffered with 6 concentric layers of brittle failure by exposing more damage diameter. The ALON 15 specimen shown in **Figure 16 (d)** succumbs to lesser percentage of failure

by rebounding the impact caused by its improved stiffness offered by the ALON particles. **Figure 16 (b) and Figure 16 (c)** express their improved elastic energy, subsequently experiences the moderate percentage of damage owing to their absorbed energy. The importance of the inclusion of ALON particles is realized through **Figure 17.** The absence of impact resistant ALON particles allows the absorbed energy to pass through the thick of the material, and causes to brittle failure on the rear side of the impact. The image clearly shows the front side indentation through fractured epoxy matrix visible in rear side.

Figure 17. Brittle failure of epoxy on the rear side of impact observed for the ALON 0-Kevlar

4.6. Dynamic Mechanical Analysis

Dynamic mechanical analysis is a technique used to examine how a material converts mechanical energy into heat energy under specific loading conditions. It assesses how materials respond to changes in frequency and temperature by analyzing storage modulus, loss modulus, and damping. Dynamic mechanical analysis is commonly employed to study the viscoelastic behavior of materials and is considered a valuable method for characterization. Storage modulus indicates a material's ability to accumulate elastic energy, while loss modulus measures its capacity to dissipate heat energy. Damping, expressed as the tangent of the phase angle (Tan δ), describes a material's ability to absorb energy and is determined by the ratio of loss modulus to storage

modulus. The experimental values of storage modulus, loss modulus, and damping for all ALON varied composites including ALON free specimens are presented in Error! eference source not found.. The properties of the materials are evaluated at three representative temperatures: 40°C, 70°C, and 180°C. The assessment of different properties at these temperatures is crucial, with 40°C chosen as the first representative temperature due to its significance near to ambient temperature. The glass transition temperature of the epoxy matrix is approximately 70°C, making it the second representative temperature. Intermediate temperatures are considered to better understand how the composite stores and dissipates energy. Therefore, a maximum temperature of 180°C is chosen. Additionally, assessing the response of the composites at the higher end of the temperature range is important to determine the stability provided by the constituents, leading to the selection of 180°C as the third representative temperature.

Table 5. Experimentally observed storage, loss modulus and tan δ value at three different temperatures

Composition	Storage Modulus (GPa)			Loss Modulus (GPa)			Tan δ		
	40 °C	70 °C	180 °C	40 °C	70 °C	180 °C	40 °C	70 °C	180 °C
ALON 0	14.82	14.09	0.597	4.94	5.033	0.094	0.0185	0.0105	0.46
ALON 5	16.60	15.78	0.067	5.53	5.67	0.105	0.0093	0.01	0.44
ALON 10	19.91	18.94	0.079	6.63	7.22	0.14	0.0082	0.0094	0.436
ALON 15	22.76	21.8	0.121	7.58	7.78	0.44	0.0078	0.84	0.857

4.6.1. Storage modulus (SM)

At the three representative temperatures shown in **Figure 18,** the composites exhibit higher storage modulus values compared to the ALON free Kevlar epoxy specimens, indicating the superior ability of ALON particles to store elastic energy under varying temperatures. Specifically, the ALON 15 composites display significantly higher storage modulus values across all representative temperatures, with an increase ranging from 12% to 53% observed at the representative temperature of 70°C. This rise in storage modulus around the glass transition temperature of the epoxy matrix can be primarily attributed to the higher proportion of the ALON particles, which imposes greater hindrance on the polymer chain mobility, enabling the composites to store more elastic energy [24, 25]. The enhanced bonding between the ALON particles and epoxy, Kevlar also contributes to the increase in storage modulus for the composites. However, at the

representative temperature of 180°C, the storage modulus of all specimens' decreases, indicating a drastic reduction in the ability to store elastic energy due to the phase transition from the glassy to rubbery region.

The results demonstrate that the storage modulus (SM) increases with the addition of ALON particles, particularly in the glassy region, and the ALON 15 composite exhibits the highest value. The incorporation of ALON particles improve the cross-linking density of the composites and restricts the mobility of the epoxy chain. This increase in SM signifies enhanced stiffness and improved bonding between the matrix and particulates. The slope of the transition region indicates the relaxation of the amorphous region and the transition from a solid to a rubbery state, where the epoxy loses its ordered arrangement [26]. The sudden decrease in SM at 70°C suggests that the addition of ALON particles has no effect at higher temperatures and highlights 70°C as the operating temperature. In the rubbery region, the inclusion of ALON particles has minimal impact, indicating a loss of bonding after the glass transition temperature and behaving more like a liquid material [27].

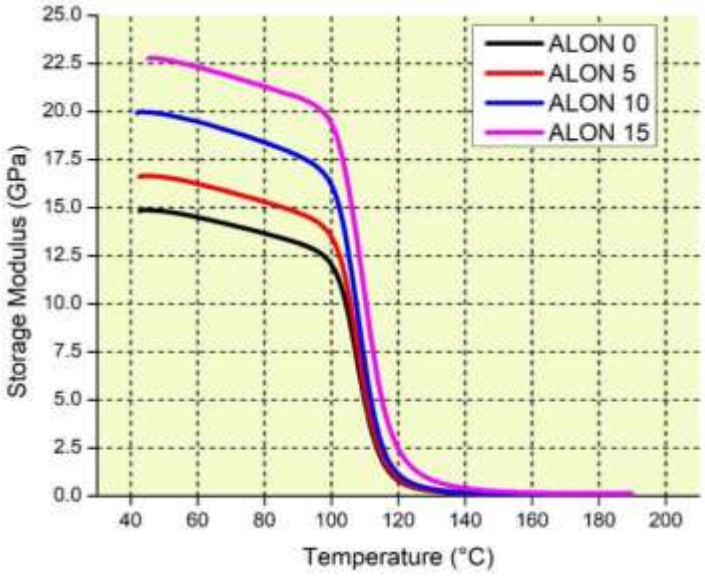

Figure 18. Storage modulus of ALON-Kevlar epoxy composite

4.6.2. Loss Modulus

Similar to the trends observed in the storage modulus, the loss modulus of the composites

also demonstrates a higher capacity for heat dissipation with increased reinforcement of the ALON particles. The ALON 15 composites exhibit higher loss modulus values at the three representative temperatures compared to other compositions, indicating their superior ability to dissipate heat energy and facilitate effective molecular readjustments during deformation [28]. From **Figure 19**, an increase ranging from 10.69 % to 63% is observed in the loss modulus of ALON 15 composites at representative temperature of 70^0C. This increase can be primarily attributed to the ability of ALON particles to absorb more energy as heat through internal friction between the constituents [29]. Additionally, ALON 15 composites effectively restrict the flow of the matrix, resulting in higher loss modulus values. On the other hand, ALON 5, ALON 10, and ALON 0 exhibit lower moduli as they offer less resistance to limit the viscosity of the matrix compared to ALON15.

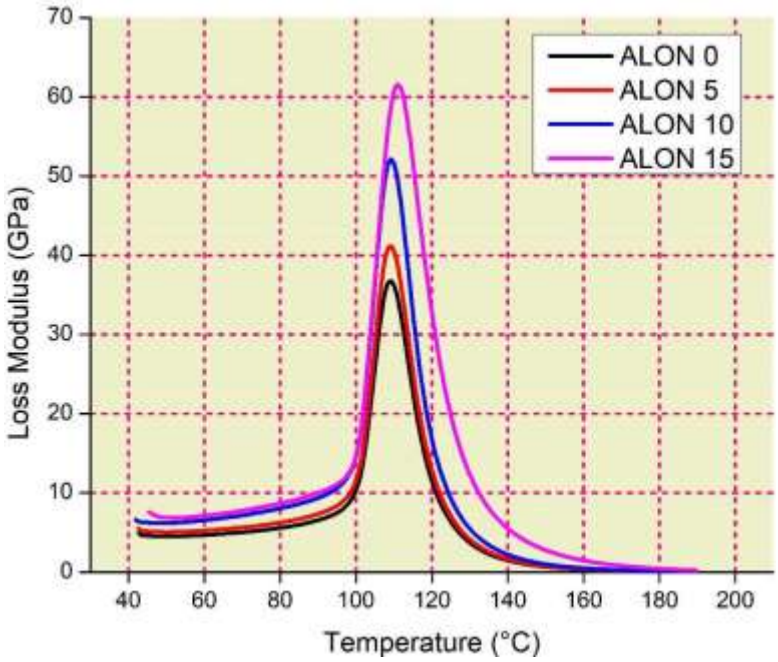

Figure 19. Loss modulus of ALON-Kevlar epoxy composite

The observed loss modulus values represent the heat dissipated due to frictional resistance, interface friction, or molecular movement at the interface between the matrix and filler. These values indicate an increasing trend in the loss modulus along with higher glass transition temperature (Tg), suggesting a greater amount of bonding between the filler and matrix. The area under the loss modulus curves varies with the increasing

content of ALON particles, and it is evident that the area is higher for ALON 15 composites [30]. The observed peaks in the curves indicate a reduction in material stiffness due to the elevated temperature, resulting in increased molecular friction at the interface. These peaks are considered as the Tg at the interfaces. As the temperature continues to rise, the friction decreases, leading to a reduction in the peak [31].

4.6.3. Damping

Figure 20 depicts that the ALON 15 composites exhibit a higher damping ratio compared to other compositions, indicating their superior damping capability. At the representative temperature of 40°C, the ALON 0 specimens have lower damping values in comparison to the composites. However, at the representative temperature of 70°C, the damping values for all the composites decrease significantly, indicating the effective energy absorption ability of ALON particles.

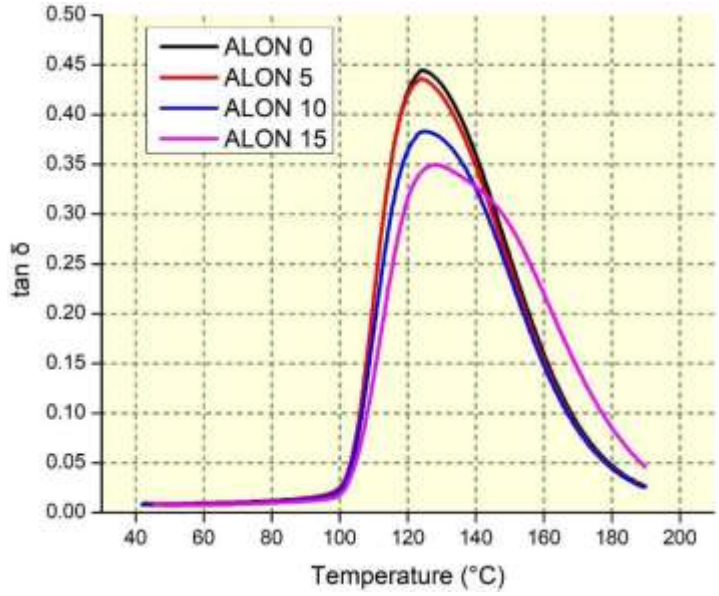

Figure 20. experimentally observed tanδ of ALON-Kevlar epoxy composite

Lower damping values indicate more elastic behavior, while higher values indicate greater damping. The addition of ALON particles to the epoxy has reduced the peak damping of the composites, but the damping remains sustained for ALON 15 at higher temperatures. This suggests that the ALON 15 composites maintain vibration effectively at elevated temperatures. Due to its higher storage modulus (SM) and loss modulus (LM), the ALON 15 composite exhibits better damping characteristics.

Additionally, the area under the damping curves for ALON 15 composites decreases with increasing temperature compared to other configurations. Generally, a decrease in the plot area is associated with improved stability of composites or materials [32, 33]. Therefore, it can be inferred that the stability of composites with ALON 15 is higher at elevated temperatures.

5. Conclusions & Recommendations

The objective of the study to develop impact and shock resistance light weight polymer composite to cater the needs of defense application, wherein sophisticated heavier materials are in use. The implementation of novel Kevlar fabric composite reinforced with ALON particles can be recommended with following results arrived through various mechanical and impact testing.

1. The SEM micrograph obtained after fabrication ensures the homogeneous dispersion of ALON particles in the matrix.
2. The tensile test results manifest the greater attainment of tensile strength of 7.68 GPa for ALON 15 specimen. In comparison with the ALON –free specimen, ALON 15 specimen records 175 % more stiffness. The tensile modulus also linearly improved with every incremental step of ALON.
3. The three-point bending experiment explores the 253 % and 159 % improvement for ALON 15 specimen than the ALON-free specimen anticipating flexural strength and flexural modulus respectively.
4. The impact results annunciate the higher impact resistance capacity of ALON 15 specimen owing to its improved stiffness.
5. The ALON particles inclusion instigates more elastic energy to rebound the impact, subsequently absorbing lesser energy responsible for the damage.
6. The failure mechanism investigated by both SEM and optical microscope reveals the sequence of failure which starts from brittle failure of the epoxy matrix, propagation of fracture induces the delamination followed by failure of Kevlar fiber.
7. The improved stiffness is further validated at high temperatures through DMA analysis. The results express a greater improvement in storage modulus, loss modulus and damping index. The results prove the ALON 15 specimen is the right candidate to function as impact resistance material in any kind of loading even at high temperature environment also.
8. The authors recommend the material to serve against functional impact loading with the requirement of lesser specific weight. The proposed materials uphold the better indices of mechanical strength and impact strength than the existing

ballistic Kevlar fabric, hence it can be suited for light weight ballistic applications also.

References

1. Grębowski, K. and M. Zielińska, *Modelling of laminated glass PVB walls of buildings exposed to vehicle impact with different speeds.* Engineering Structures, 2023. **292**: p. 116494.
2. Minor, J.E., *8 - Glazing systems to resist windstorms on special buildings*, in *Architectural Glass to Resist Seismic and Extreme Climatic Events*, R.A. Behr, Editor. 2009, Woodhead Publishing. p. 217-231.
3. Wright, S.C., N.A. Fleck, and W.J. Stronge, *Ballistic impact of polycarbonate—An experimental investigation.* International Journal of Impact Engineering, 1993. **13**(1): p. 1-20.
4. Ilya, K., et al., *Development thermoplastic elastomer-based fiber-metal laminate for vibration damping application.* Materials Today: Proceedings, 2020. **30**: p. 393-397.
5. Reis, P., et al., *Impact response of Kevlar composites with filled epoxy matrix.* Composite Structures, 2012. **94**(12): p. 3520-3528.
6. Sharma, S., et al., *Excellent mechanical properties of long multiwalled carbon nanotube bridged Kevlar fabric.* Carbon, 2018. **137**: p. 104-117.
7. Wang, Y., J. Li, and D. Zhao, *Mechanical properties of fiber glass and kevlar woven fabric reinforced composites.* Composites Engineering, 1995. **5**(9): p. 1159-1175.
8. Audibert, C., et al., *Mechanical characterization and damage mechanism of a new flax-Kevlar hybrid/epoxy composite.* Composite Structures, 2018. **195**: p. 126-135.
9. Zhang, Z.T., et al., *Manufacture and properties of AlON-TiN particulate composites.* Key Engineering Materials, 2004. **280**: p. 1133-1138.
10. Avila, A.F. and D.T. Morais, *Modeling nanoclay effects into laminates failure strength and porosity.* Composite structures, 2009. **87**(1): p. 55-62.

11. Avila, A.F., M.I. Soares, and A.S. Neto, *A study on nanostructured laminated plates behavior under low-velocity impact loadings.* International journal of impact engineering, 2007. **34**(1): p. 28-41.
12. Priyanka, P., H.S. Mali, and A. Dixit, *Dynamic mechanical behaviour of kevlar and carbon-kevlar hybrid fibre reinforced polymer composites.* Proceedings of the Institution of Mechanical Engineers, Part C: Journal of Mechanical Engineering Science, 2021. **235**(19): p. 4181-4193.
13. Madarvoni, S. and S. PS Rama, *Dynamic mechanical behaviour of graphene, hexagonal boron nitride reinforced carbon-kevlar, hybrid fabric-based epoxy nanocomposites.* Polymers and Polymer Composites, 2022. **30**: p. 09673911221107289.
14. Sarasini, F., et al., *Drop-weight impact behaviour of woven hybrid basalt–carbon/epoxy composites.* Composites Part B: Engineering, 2014. **59**: p. 204-220.
15. Chenrayan, V., et al., *Experimental and numerical assessment of the flexural response of banana fiber sandwich epoxy composite.* Scientific Reports, 2023. **13**(1): p. 18156.
16. Hebert, M., C.-E. Rousseau, and A. Shukla, *Shock loading and drop weight impact response of glass reinforced polymer composites.* Composite structures, 2008. **84**(3): p. 199-208.
17. Richard, S., J. Selwin Rajadurai, and V. Manikandan, *Effects of particle loading and particle size on tribological properties of biochar particulate reinforced polymer composites.* Journal of Tribology, 2017. **139**(1).
18. Basavarajappa, S., et al., *Three-body abrasive wear behaviour of polymer matrix composites filled with SiC particles.* Polymer-Plastics Technology and Engineering, 2009. **49**(1): p. 8-12.
19. Patel, J.S., et al., *Effect of fabric structure and polymer matrix on flexural strength, interlaminar shear stress, and energy dissipation of glass fiber-reinforced polymer composites.* Textile Research Journal, 2016. **86**(2): p. 127-137.
20. Gossaye, K., et al., *Compressive behavior of Habesha eggshell particulate reinforced epoxy composites.* Polymer Composites, 2023.

21. Bowlby, L.K., G.C. Saha, and M.T. Afzal, *Flexural strength behavior in pultruded GFRP composites reinforced with high specific-surface-area biochar particles synthesized via microwave pyrolysis.* Composites Part A: Applied Science and Manufacturing, 2018. **110**: p. 190-196.
22. Mohanty, A. and V. Srivastava, *Effect of alumina nanoparticles on the enhancement of impact and flexural properties of the short glass/carbon fiber reinforced epoxy based composites.* Fibers and Polymers, 2015. **16**(1): p. 188-195.
23. Belingardi, G. and R. Vadori, *Low velocity impact tests of laminate glass-fiber-epoxy matrix composite material plates.* International Journal of Impact Engineering, 2002. **27**(2): p. 213-229.
24. Karsli, N.G. and A. Aytac, *Tensile and thermomechanical properties of short carbon fiber reinforced polyamide 6 composites.* Composites Part B: Engineering, 2013. **51**: p. 270-275.
25. Doddamani, M., *Dynamic mechanical analysis of 3D printed eco-friendly lightweight composite.* Composites Communications, 2020. **19**: p. 177-181.
26. Yang, M., et al., *Thermal and mechanical performance of unidirectional composites from bamboo fibers with varying volume fractions.* Polymer Composites, 2019. **40**(10): p. 3929-3937.
27. Dayo, A.Q., et al., *Natural hemp fiber reinforced polybenzoxazine composites: Curing behavior, mechanical and thermal properties.* Composites Science and Technology, 2017. **144**: p. 114-124.
28. Gu, J., G. Wu, and Q. Zhang, *Effect of porosity on the damping properties of modified epoxy composites filled with fly ash.* Scripta materialia, 2007. **57**(6): p. 529-532.
29. Lewis, T. and L. Nielsen, *Dynamic mechanical properties of particulate-filled composites.* Journal of applied polymer science, 1970. **14**(6): p. 1449-1471.
30. Sahoo, S.K., S. Mohanty, and S.K. Nayak, *Mechanical, thermal, and interfacial characterization of randomly oriented short sisal fibers reinforced epoxy composite modified with epoxidized soybean oil.* Journal of Natural Fibers, 2017. **14**(3): p. 357-367.

31. Oboh, J., et al., *Dynamic mechanical properties of crosslinked natural rubber composites reinforced with cellulosic nanoparticles.* Nigerian journal of technology, 2018. **37**(3): p. 668-673.
32. Doddamani, M., *Effect of surface treatment on quasi-static compression and dynamic mechanical analysis of syntactic foams.* Composites Part B: Engineering, 2019. **165**: p. 365-378.
33. Shunmugasamy, V.C., D. Pinisetty, and N. Gupta, *Viscoelastic properties of hollow glass particle filled vinyl ester matrix syntactic foams: effect of temperature and loading frequency.* Journal of Materials Science, 2013. **48**: p. 1685-1701.

Approval of investigators

We hereby declare that research report entitled "**Development and Performance Evaluation of Impact and shock resistant wallpaper for Defense application**" Is our original work; all sources are duly acknowledged and report is compiled by incorporating the necessary comments and suggestions given by the reviewers.

	Name	Signature	Date
Principal Investigator	Dr. Kiran Shahapurkar		15/02/2024
Co-Investigator	Dr. Venkatesh Chenrayan		15/02/2024
Co-Investigator	Mr. Girmachew Ashegiri	_____	_____

Approval of Reviewers

I hereby confirm that (PI) Dr. Kiran Shahapurkar has accomplished his/her work as per the approved proposal and incorporated all the comments given by the reviewers in his terminal report of the project entitled "**Development and Performance Evaluation of Impact and shock resistant wallpaper for Defense application"** and hence the report qualifies for submission as standard research output.

	Name	Signature	Date
Reviewer 1.	_____	_____	_____
Reviewer 2.	_____	_____	_____

Approval: School Ethical Review Board (SERB)

	Name	Signature	Date
1.			
2.			
3.			
4.			